INVITED PAPER

Chemical Recognition With Broadband THz Spectroscopy

T-rays can be used to probe biochips, to perform biosensing and chemical sensing, and to identify many crystalline substances, but amorphous substances are more difficult to identify.

By Bernd M. Fischer, Hanspeter Helm, and Peter Uhd Jepsen

ABSTRACT | THz science is developing rapidly in Europe as well as the rest of the world. There is a strong interest in the exploitation of optical technologies in the THz frequency range in virtually all fields of basic and applied sciences of physics, chemistry, biology as well as medicine. Commercial interest in this field has also been growing, spurred by the potential of THz tools in quality control and the biotechnology sector. We will review some contrast mechanisms, which form the basis for real-world applications of THz technology, in particular in the fields of applied chemistry and biotechnology. Whereas narrow bandwidth THz technology may become important for, e.g., real-time imaging at larger standoff distances, we will concentrate on broad bandwidth THz technologies for spectroscopic identification of various substances. It has recently been established that the 0.1–5 THz spectral range contains unique fingerprints of a very large number of crystalline materials, including explosives, illicit drugs as well as most other chemicals in powder form. Since many packaging materials are transparent to THz radiation this fundamental property of crystalline compounds allows remote (contact-free) sensing combined with chemical recognition. On the other hand, the THz spectrum of amorphous systems, including aqueous solutions, contains very little information about the detailed composition of the system. However, under certain conditions it is still possible to learn a great deal about amorphous systems with broadband THz spectroscopy. Amorphous systems of great biotechnological importance include DNA and proteins, both in aqueous solution and as dried matter. We will discuss methods for THz science and technology to attack the very complex problems involved in the extraction of useful new information, which may be difficult, expensive, or impossible to obtain with other methods, from minute amounts of biomaterial.

KEYWORDS | Chemical recognition; THz-imaging; THz-TDS

I. INTRODUCTION

In recent years, there has been an increased interest in understanding the response of matter to electromagnetic radiation in the THz-frequency range. Among the many possible avenues of application of THz radiation is the interest in detecting and characterizating biological material. Of particular interest are the molecular response of biological material to electromagnetic radiation [1]–[3], the radiation signatures of low-frequency vibrations in RNA- and DNA strands [4], [5] and proteins [6], [7], as well as the power of this frequency window to act as diagnostic sensor, such as the detection of skin cancer by THz imaging [8].

A different avenue of application arises in the safety/security sector. Most nonpolar nonmetallic packaging materials are transparent at terahertz frequencies, thus enabling THz radiation to penetrate through concealing barriers, in order to identify crystalline and in particular potentially dangerous materials inside sealed environments. Progress in this technology now promises realistic applications based on chemical recognition in identifying explosives [9] and biological agents [10], a matter greatly stimulating commercial interest in THz technologies.

Manuscript received October 7, 2005; revised March 27, 2007. This work was supported in part by the IEEE, in part by BMBF and the EU project THz-BRIDGE under Contract QLK4- CT-2000-00129, and in part by project start-up funds from Albert Ludwigs University under Grant ZEE20030131.

B. M. Fischer is with the Department of Molecular and Optical Physics, Freiburg Materials Research Center, Universität Freiburg, D-79104 Freiburg, Germany, and also with the School of Electrical and Electronic Engineering and Centre for Biomedical Engineering, University of Adelaide, Adelaide SA 5005, Australia (e-mail: bernd.fischer@adelaide.edu.au).

H. Helm is with the Department of Molecular and Optical Physics, Freiburg Materials Research Center, University of Freiburg, D-79104 Freiburg, Germany.

P. U. Jepsen is with the Department of Molecular and Optical Physics, Freiburg Materials Research Center, University of Freiburg, D-79104 Freiburg, Germany, and also with the Department of Communications, Optics, and Materials, Technical University of Denmark, DK-2800 Kongens Lyngby, Denmark.

Digital Object Identifier: 10.1109/JPROC.2007.898904

In this contribution we will concentrate on broad bandwidth spectroscopic identification of a wide range of fundamental substances of interest. Frequency-resolved spectral information obviously forms the basis for single-frequency applications. Our work centers on pulsed THz-spectroscopy, which is based on the generation and detection of ultrashort and coherent electromagnetic pulses in the very-far-infrared range. The subpicosecond duration of the pulses results in a bandwidth covering the region from 0.1 to 5 THz of the electromagnetic spectrum. Broadband detection schemes can be applied in this range which help to distinguish between richly structured spectra and therefore enabling identification by comparison with the entries in a database.

Distinct spectral signatures in the THz absorption spectrum of a substance are intimately connected to the underlying molecular long-range order. Substances in the condensed phase are held together by either ionic, covalent or electrostatic forces, and therefore the lowest frequency modes will be associated with intermolecular motion. A medium with long-range ordering of its molecular constituents can support phonon-like intermolecular modes at discrete frequency bands, whereas an amorphous medium will display a continuum of strongly damped intermolecular vibrational modes. At higher frequencies, where intramolecular modes are active, this picture is no longer valid. Here, the vibrational modes of the isolated molecules are found, albeit influenced by the surroundings. Easy experimental examples can directly demonstrate the intermolecular character of the molecular vibrations that lead to the characteristic bands observed in the THz spectra. On the other hand, the THz spectrum of amorphous systems, including aqueous solutions, contains very little information about the detailed composition of the system. Amorphous systems of great biotechnological importance include DNA and proteins, both in aqueous solution and as dried matter. Under controlled conditions, it is still possible to use broadband THz spectroscopy to distinguish between such materials, despite the lack of sharp clear resonance features.

II. EXPERIMENTAL

The dielectric properties of the samples presented in this work are studied using terahertz time-domain spectroscopy (THz-TDS). The generation and the detection of THz radiation is based on photoconductive switches. The dielectric function of a material is determined in transmission THz-TDS by measuring a reference pulse $E_{\mathrm{ref}}(t)$ propagating through an empty spectrometer and a sample pulse $E_{\mathrm{sam}}(t)$ propagating through the spectrometer with the sample of thickness d placed in the beam path. The field of the THz pulse transmitted through the sample $E_{\mathrm{sam(t)}}$ is modified by the dispersion $n(\nu)$ and absorption $\alpha(\nu)$ of the sample. The temporal shape of the two pulses is transformed into the frequency domain, and the amplitude $A(\nu)$ and phase $\Phi(\nu)$ of the ratio of the two spectra

$$\frac{E_{\mathrm{sam}}(\nu)}{E_{\mathrm{ref}}(\nu)} = \frac{4n}{(n+1)^2}\exp[-\alpha d/2 + i2\pi\nu(n-1)d/c] = A(\nu)\exp[i\Phi(\nu)] \quad (1)$$

are calculated and analyzed to obtain the spectra of the absorption coefficient

$$\alpha(\nu) = -\frac{2}{d}\ln\left\{A(\nu)\frac{[n(\nu)+1]^2}{4n(\nu)}\right\} \quad (2)$$

and the index of refraction

$$n(\nu) = 1 + \frac{c}{2\pi\nu d}\Phi(\nu). \quad (3)$$

In Fig. 1(b) a typical THz pulse is shown together with its frequency spectrum. Owing to the typical single-cycle nature of the THz pulse, its frequency spectrum extends from the low gigahertz region up to several THz. At high frequencies the spectrum is characterized by a gradual roll-off, until the detected signal level approaches that of the noise floor of the experiment.

In order to record the temperature dependence of the spectral features the samples are mounted in a cryostat equipped with TPX [11] windows. The temperature is measured near the sample by a calibrated Si-diode with an accuracy of ± 1 K. The cryostat can be moved so that the THz beam passes through either the sample or through an empty aperture of the identical size as the clear aperture of the sample.

III. CRYSTALLINE SAMPLES

The terahertz spectra of polycrystalline samples of molecules of biological relevance are dominated by sharp distinct characteristic bands, showing a pronounced sensitivity upon small changes in the molecular structure. Thus, THz-spectroscopy can be applied to distinguish between similar molecules of the same class of biomolecules [12]–[14] and even between isomeric configurations [15]–[17] by their terahertz signature. Due to this pronounced specificity the THz spectral range is often referred to as a fingerprint region. THz-TDS offers a relatively easy and convenient technique to record the far-infrared spectra. The fact that in particular pharmaceuticals [18], [19], illicit drugs [20], [21], and explosives [22], [23] show such characteristic spectra indicates the

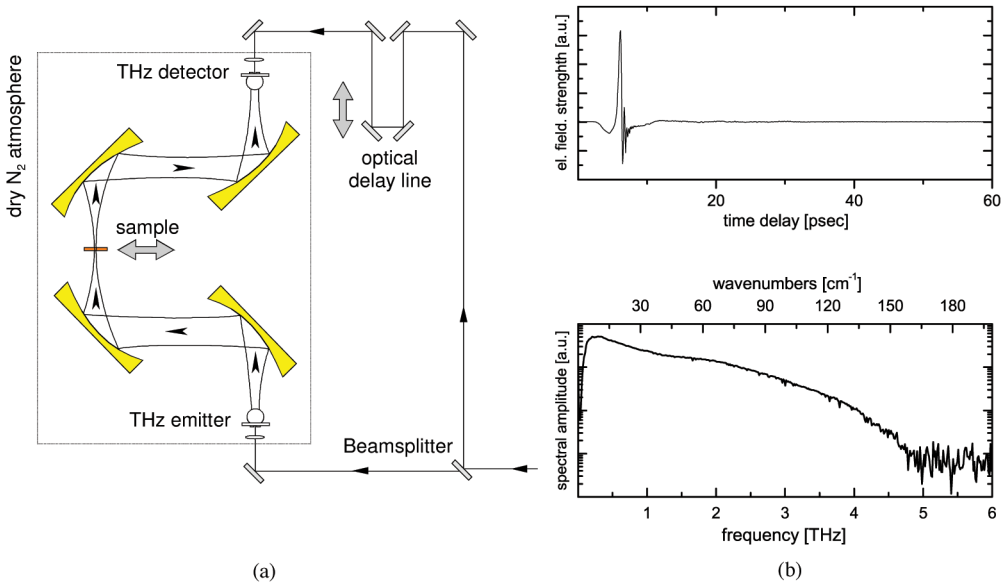

Fig. 1. *(a) Schematic diagram of a THz time-domain spectromete. (b) Temporal shape of a THz-pulse and corresponding frequency spectrum.*

enormous potential this technique holds for applications based on spectral recognition.

In this work we present four new examples to demonstrate the individuality of the terahertz spectra of these classes of substances. In Fig. 2 we show the absorption spectra of α-D-glucose, β-D-glucose, testosterone, and 1,3,-dinitrobenzene, recorded at ambient temperature (dashed lines) and cooled to 13 K (solid lines). The powdery polycrystalline sample material was mixed with PE and pressed to pellets to ensure physical stability and planar interfaces.

Carbohydrates are an important class of biomolecules [24], as they make up most of the organic material and because of their multiple roles in energy stores, structural elements and framework for DNA, cellwalls, proteins, and lipids. The study of the far-infrared dielectric properties of carbohydrates has been subject of several recent publications [16], [17], [25]. The high sensitivity of the spectra to small changes in the molecular structure enables even a differentiation between the spectra of the glucose anomers, as shown in Fig. 2(a) and (b). While some similarities in the spectra are observed—for example the first strong modes are only slightly shifted to higher frequencies in the β-anomer—clear differences appear in the range between 50 cm^{-1} and 75 cm^{-1}.

Most pharmaceuticals are of polycrystalline constitution and show characteristic terahertz absorption spectra that can be used to fingerprint and thereby probe the purity of a medically active agent or to identify illicit drugs [20], [21]. In Fig. 2(c) the absorption spectrum of the male hormone testosterone is shown, showing several strong sharp bands in the entire frequency range investigated.

The capability of contact-free crystalline substances identification by their spectroscopic fingerprints is of particular interest in safety and security applications. An extended catalogue of terahertz spectra of most common explosives has been recorded [26] in the last three years. In Fig. 2(d) we show the absorption spectrum of 1,3-dinitrobenzene (DNB). In the low frequency range several sharp absorption peaks are observed. At frequencies above 1.6 THz a pronounced increase of the signal is observed before the dynamic limit [27] in this particular sample is reached at approximately 2 THz. The very sharp bend of the absorption curve, followed by the unspecific roll-off of the signal [shown as gray dots in Fig. 2(d)] indicates that the measured absorption coefficient can only be trusted until the detection limit set by the dynamic range is met.

IV. THEORETICAL PREDICTIONS OF FAR-INFRARED SPECTRA

In the last few years, density functional theory (DFT) has proven to be a reliable theoretical method to predict accurate vibrational frequencies for medium sized molecules [28]–[30]. The intermolecular character of the low-frequency vibrations has yet to be considered in detail. We have recently reported DFT calculations of thymine molecular structures [20]. The calculated vibrational properties of a single molecule are in no way related to the observed spectrum. Only when considering a hydrogen-bridge bound compound of molecules arranged in space according to the crystallographic data [31] the calculations predict bands which are similar to the

experimental data. Therefore, the inclusion of periodic boundary conditions in the calculation of vibrational frequencies will definitely help to improve the assignment capabilities.

Alternatively, molecular mechanics calculations with adapted force fields have in some situations shown good agreement with experimental spectra of crystalline organic compounds [32], [33]. The success of this approach depends strongly on an adaptation of the force field parameters to the specific molecule in order to reproduce the experimental vibrational spectrum. Thus, in spite of the good agreement with experiment that can be obtained, this method has limited predictive strength for molecular systems to which the force field has not been adapted. On the other hand, if a force field valid for a broad range of compounds can be found, then this method holds the potential for prediction of far-infrared vibrational spectra.

V. DIRECT EXPERIMENTAL OBSERVATION OF THE INTERMOLECULAR CHARACTER OF THE TERAHERTZ MODES

Most calculations of the terahertz spectra indicate that the molecular vibrations that give rise to the characteristic spectral features of polycrystalline samples are of intermolecular character. In some cases this can be directly demonstrated by comparing spectra of a sample in different constitution. We propose three simple experiments that indicate the intermolecular character of the terahertz spectra of polycrystalline samples.

A. Crystalline and Amorphous Glucose

To some extent sugars represent prototype systems of hydrogen-bonded networks both in the crystalline and in the amorphous state. In the solid state saccharides are linked by a rigid network of hydrogen bonds which in crystals are of long range order [34], resulting in highly

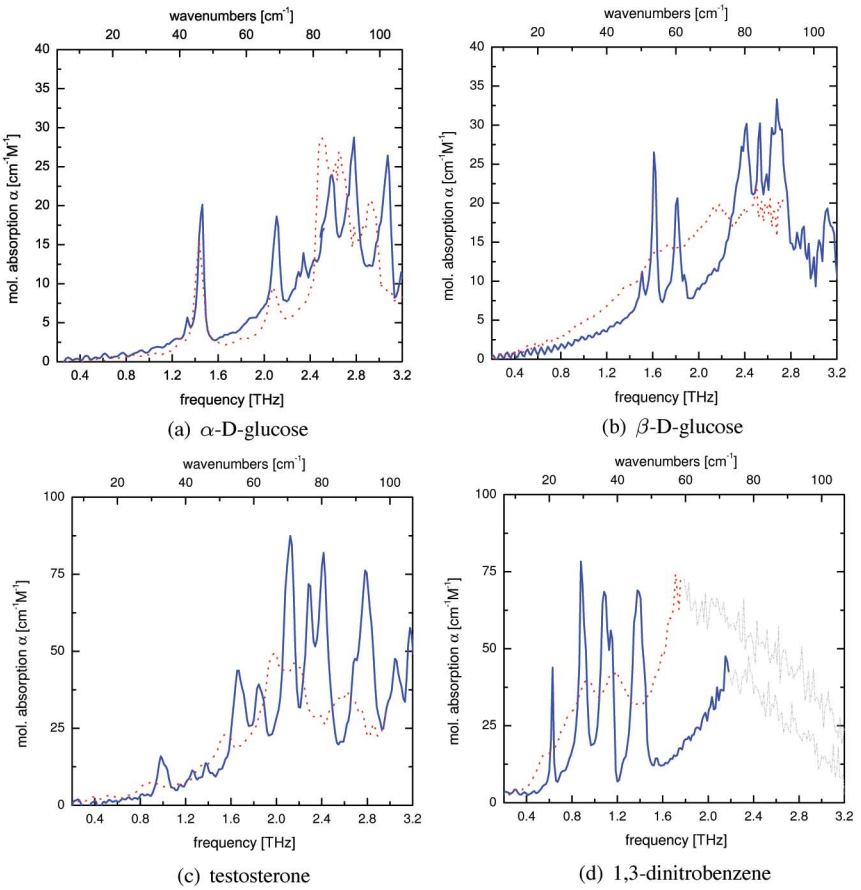

Fig. 2. *Molar absorption of α-D-glucose, β-D-glucose, testosterone, and 1,3-dinitrobenzene (DNB), recorded at room temperature (dashed lines) and cooled to 13 K (solid lines). All spectra show very characteristic absorption features that can be used for fingerprint. Due to the strong absorption of DNB at high frequencies, the signal grows until the dynamic range of the experiment is reached at frequencies of approximately 2 THz. The very sharp bend of the absorption curve at this point and the following roll-off of the signal show that the measured absorption coefficient can only be trusted up to the detection limit set by the dynamic range. (a) α-D-glucose. (b) β-D-glucose. (c) Testosterone. (d) 1,3-dinitrobenzene.*

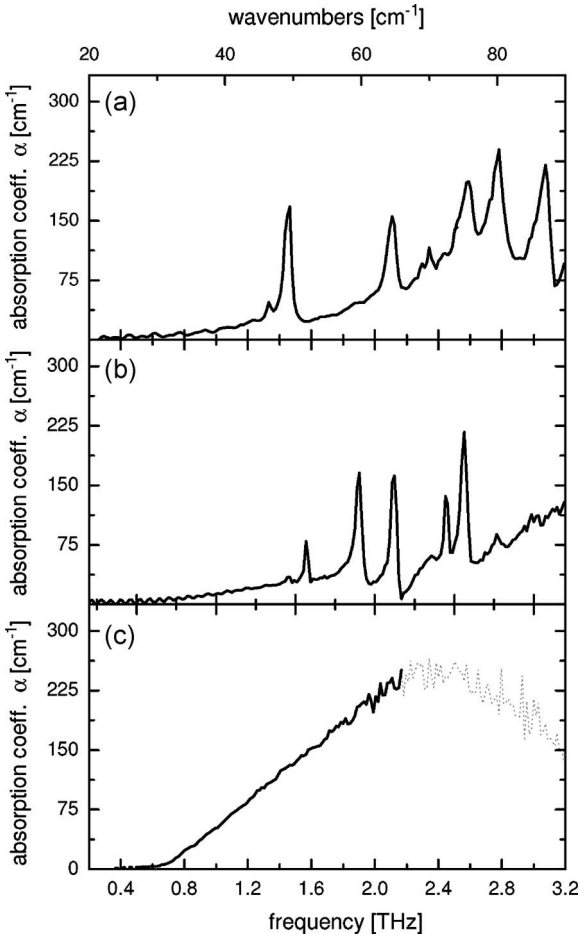

Fig. 3. ***Absorption spectra of: (a) polycrystalline α-D-Glucose, (b) polycrystalline α-D-glucose monohydrate, and (c) amorphous D-glucose. While the spectra of the polycrystalline samples are dominated by sharp characteristic resonance bands, the spectrum of the amorphous sample shows no distinct features.***

regular lattice vibrations, or phonon modes, of the entire crystal structure. In Fig. 3 we compare the spectra of polycrystalline α-D-glucose, polycrystalline α-D-glucose monohydrate, and amorphous glucose. The polycrystalline samples were again prepared by diluting the powdery material in PE and pressing this mixture in a die using a hydraulic press to stable coplanar pellets. The amorphous sample was prepared by melting of polycrystalline glucose followed by rapid cooling of the sample material between two cold glass plates. The rapid cooling inhibits recrystallization of the sugar.

The incorporation of a water molecule in the monohydrate crystal has obviously a strong impact on the intermolecular hydrogen bonds: the central molecule is hydrogen-bonded to 12 glucose molecules in the anhydrous crystal structure and to six glucose molecules and four water molecules in the monohydrate. The intramolecular bonds remain nearly undisturbed [34], [35]. Yet the absorption spectra of anhydrous and monohydrated glucose differ significantly from each other. In contrast, in the spectrum of amorphous glucose a featureless absorption profile appears with monotonously increasing absorption at high frequencies.

The differences of the dielectric properties of anhydrous, monohydrated, and amorphous glucose lead us to conclude that the sharp spectral features observed in the polycrystalline sugars arise from concerted intermolecular vibrational modes of long-range order, controlled by noncovalent bonds between the sugar molecules. Due to the lack of long-range symmetry, all sharp spectral features disappear in amorphous glucose, but absorption is still considerable due to the now random orientation of intermolecular bonds. If intramolecular vibrational modes were present in the frequency range considered here, such modes should be visible in the spectra of the amorphous sugars.

B. Tartaric Acid

A further simple experiment which can be used to classify the origin of the low-frequency resonances observed in polycrystalline samples is the comparison of different crystalline configurations of tartaric acid. Tartaric acid is an important additive in foods and pharmaceuticals. The structures of its various forms are of historical interest, dating back to the pioneer work of Pasteur (1848, 1850). The form of its natural appearance is the L(+) enantiomer. The dielectric properties in the far-infrared are—due to the symmetry of the molecular structure—identical for enantiomers. In Fig. 4 the absorption spectrum of the racemic mixture (a), an equal mixture of polycrystalline L(+) and D(−)-tartaric acid is compared to the spectrum of the racemic compound DL(±)-tartaric acid (b), which is crystallized with the pairs of L- and D-tartaric acid molecules. Both spectra show several distinct absorption peaks. Yet whereas the spectra of the pure enantiomers show a strong pronounced peak at 35 cm^{-1} followed by a series of sharp bands, the spectrum of the racemic compound shows two broad bands. In particular, the lowest mode is found at significant higher frequencies than in the spectra of the pure enantiomers. As both samples consist of the same components, the pronounced difference of the spectra directly indicates the intermolecular character of the corresponding molecular vibrations. Yamaguchi and coworkers have recently shown similar pronounced differences in the THz spectra of enantiopure and racemic polycrystalline alanine [36].

Representative for all graphs in this paper, we show error bars in Fig. 4. These error bars represent one standard deviation of the average absorption coefficient and index of refraction, calculated from the standard deviation of the average of several time-domain traces.

Tartaric acid has often been cited as a case satisfying Wallach's rule [37], [38] which states that racemic crystals tend to be denser than their chiral counterparts.

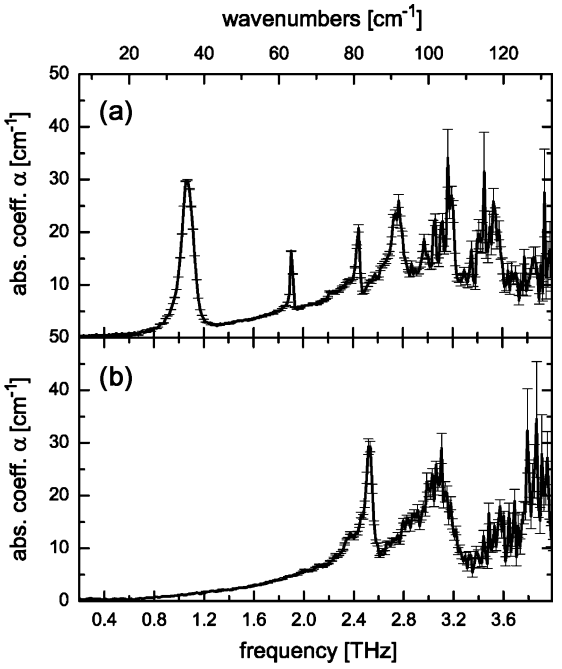

Fig. 4. *Absorption spectra of an equal mixture of L- and D- tartaric acid (racemic mixture) and DL-tartaric acid (racemic compound). Although the samples are composed of the same components, the different forms of crystallization lead to a pronounced difference in the terahertz spectra. The error bars shown in this graph are representative for all spectra of polycrystalline samples shown in this work.*

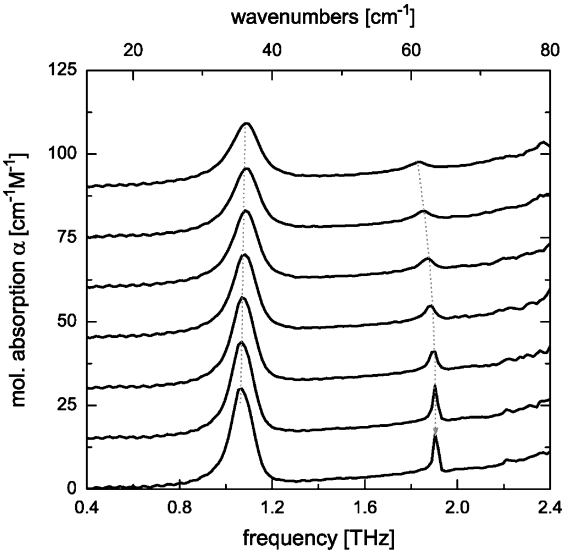

Fig. 5. *Absorption spectrum of* D(−)*-tartaric acid in the frequency range 0.4–2.4 THz, at temperatures from 13 K to 300 K. The different traces are vertically offset for a clearer representation.*

Luner *et al.* [39] reported that the racemate of tartaric acid is even significantly denser than the homochiral form. The thus stronger intermolecular bonds could explain the strong shift of the modes towards higher frequencies in the racemate. However, in some few cases, the THz spectrum of the racemate shows strong absorption features at lower frequencies than in the case of the enantiopure sample [40].

A detailed study of the temperature dependence of the absorption spectra of the pure enantiomers confirms the weak bonding forces involved. In the case of polycrystalline D(+) tartaric acid, the transition frequencies of the lowest mode is observed to shift to higher frequencies when increasing the crystal temperature, as shown in Fig. 5. Only at the highest investigated temperatures did we observe the expected redshift of the transitional frequencies as can be seen in the representation of the relative frequency shift $(\nu(T)/\nu_{13K} - 1)$ shown in Fig. 6. The absorption lines at higher frequencies all shift to lower frequencies with increasing temperature. We reported an analogous temperature dependence of the transition frequencies of the lowest modes of sucrose [16]. We tentatively interpret this unusual blueshift of the lowest transitions in tartaric acid as a direct manifestation of intermolecular forces much weaker than the hydrogen-bond network between the molecules. At low temperatures these weak forces (such as van der Waals forces) dominate over the thermal motion of the lattice, and hence they can be directional. They can lead to a softening of the intermolecular hydrogen bonds, in analog to the well-known softening of covalent bonds by the presence of hydrogen bonds, often observed in mid-IR spectroscopy [41], and used as indicator of the presence of hydrogen bonds. At higher temperatures these weak interactions are effectively switched off by thermal motion of the crystal

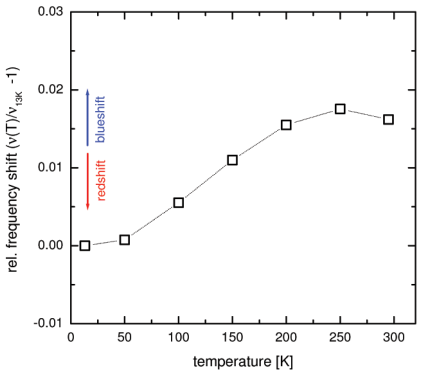

Fig. 6. *Relative shift* $\nu(T)/\nu_{13K} - 1$ *of the center frequency of the lowest resonance peak in the absorption spectrum of* D(−)*-tartaric acid. At low temperature a blueshift of the center frequency with increasing temperature is observed. At the highest only at the highest investigated temperatures the center frequency follows the typical redshift.*

lattice, leading to a tightening of the hydrogen bond and a resulting blueshift of the vibrational frequency of the bond. At still higher temperatures the nonharmonic character of the potential becomes important, and the regular redshift of the vibrational frequency is observed.

C. Chlorobenzene

In the previous examples the intermolecular character of the terahertz vibrations of polycrystalline samples was demonstrated by comparing the spectra of two different samples. At the example of chlorobenzene we present a case where the constitution the sample is changed from liquid to crystalline by lowering the temperature. We show that this change of the configuration has a tremendous impact on the THz-absorption spectra.

Chlorobenzene is a toxic aromatic compound, with the chemical formula C_6H_5Cl. The sample was prepared for spectroscopy by filling the liquid sample in a cell covered by TPX windows separated by a metal spacer of 500 μm thickness. At temperatures above the melting point at -45 °C, it is a colorless liquid, and its absorption spectrum, shown in Fig. 7, shows a broad, featureless absorption. When cooled down to temperatures below the melting point, the sample freezes out to a polycrystalline constitution, and sharp distinct absorption peaks arise in its terahertz spectrum. Analogue to the absorption features observed in crystalline samples, upon further decrease of the temperature these peaks sharpen and shift slightly towards higher frequencies, as expected for lattice bands.

In conclusion, these observation lead us to an important conclusion regarding the feasibility of THz spectroscopy for the identification of biological substances. If the substance is of crystalline nature, there is a good chance that THz spectroscopy can be used for its identification, but if the substance is of amorphous nature the specificity of the THz absorption spectrum to the individual substance is lost.

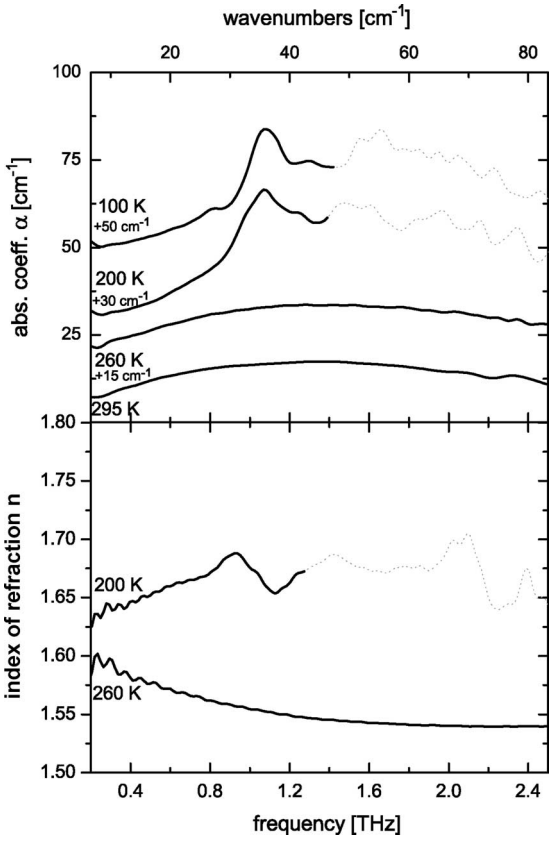

Fig. 7. *Temperature dependence of the absorption coefficient α and index of refraction of chlorobenzene. For better visibility the individual traces for the absorption coefficient are shifted vertically by an offset indicated in the figure. The index of refraction is shown representatively for two temperatures. Clear differences in the spectra of the liquid and polycrystalline samples are observed.*

VI. THz-IMAGING WITH CHEMICAL RECOGNITION

Having established that many materials have characteristic THz spectra that can be used to fingerprint and thereby identify concealed materials it is tempting to explore the potential of THz imaging for detection purposes. The potential of technical imaging in the very far-infrared (FIR) range has been considered as early as 1975 but had not been pursued past an initial proof of principle [42], due to the lack of easy-to-use sources at that time. Recent advancements in ultrashort electromagnetic pulse generation has revived this subject [11], [43]. In particular, electrooptical techniques are now capable of upconverting an FIR radiation field pattern into the visible domain [44], [45], permitting live viewing of the spatial and temporal distributions of the electric field strength. Very recently, distinction between different types of biological material in pulsed THz imaging [46], as well as detection of specific chemicals in scanning continuous-wave THz imaging [21], [47], was demonstrated.

In this work we will demonstrate that THz imaging combined with a straightforward THz-TDS analysis of the transmitted THz pulses allows contact-free and reliable recognition of chemicals hidden in containers. The applied recognition algorithm is simple and fast, and scales linearly with the number of chemical substances in the reference database. In Fig. 8 a photograph of a sample, consisting of four pellets glued to a piece of paper, is shown. Each pellet contains 60 mg of either lactose, aspirin, sucrose, or tartaric acid, mixed and pressed with 80 mg of polyethylene powder for mechanical stability. We record the full THz pulse shape (truncated 5 ps before the main pulse and with a length of 70 ps) transmitted through the sample. We use a 25 $\times$ 25 pixel grid, with a grid spacing of 2 mm. THz images can then be formed by different methods, as will be discussed below. In Fig. 9(b)

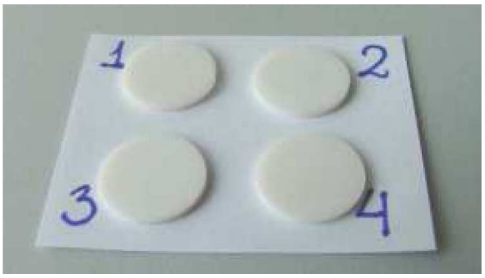

Fig. 8. *Visible image of sample with four pellets containing different chemicals: (1) lactose, (2) aspirin, (3) sucrose, and (4) tartaric acid.*

the THz transmission image of the sample is shown, obtained by recording the peak amplitude of the THz pulse after transmission through the sample, which is mounted on a 1 cm thick styrofoam plate and covered with a second sheet of paper during the measurements. The four pellets are clearly visible in the THz image, but no distinction between the chemicals is possible by this simple imaging technique. In order to identify and distinguish the chemicals in the sample, we define a recognition coefficient R proportional to the height of a spectral feature with respect to its baseline

$$R = \alpha(\nu_2) - \frac{1}{2}(\alpha(\nu_3) - \alpha(\nu_1)) \tag{4}$$

where α is the absorption coefficient. If more than one clear spectral feature is present in the absorption spectrum then R may be taken as the sum or product of several peak heights, thereby increasing the specificity. For samples of unknown thickness or irregular shape only the product $\alpha \cdot d$ is measured. In this situation, the product of absorption and sample thickness can be used in (4), as shown below. The absorption spectra of lactose, aspirin, sucrose, and tartaric acid shown in Fig. 10 are extracted from the THz pulses transmitted through the relevant regions of the sample. The solid lines show the absorption averaged over the pellet areas (20–30 pixels), with vertical bars indicating the corresponding standard deviation. The lower absorption curve in each panel shows the background absorption of the packaging material. The standard deviation is indicated for an average over 30 pixels. The vertical lines indicate the frequencies chosen for chemical recognition. In Fig. 11 maps of recognition coefficient R for the four chemicals in the sample are shown, using the frequencies indicated in Fig. 10. For aspirin and tartaric acid we use one peak for recognition, and for lactose and sucrose the sum of two peaks is used. In spite of its simplicity, the recognition strategy presented here is clearly capable of identifying the four different chemicals contained in the sample. Due to the prominent spectral features in the absorption spectra of lactose and tartaric acid, the signal-to-noise ratio of the recognition signals for those substances is strong and clear. In spite of the weak spectral features and relatively large background absorption of aspirin and sucrose the recognition strategy is still successful, although with slightly lower signal-to-noise ratio. Within the limits of the dynamical range of the spectrometer, the recognition coefficient is proportional to the concentration of the chemical. With the proper calibration, this strategy can therefore also be used to determine the concentration of the chemical. This capability has been demonstrated in experiments with quasi-continuous-wave THz radiation by Kawase and coworkers [21], [47]. We note that owing to the relatively broad line shapes in the THz absorption spectra, chemical recognition with THz

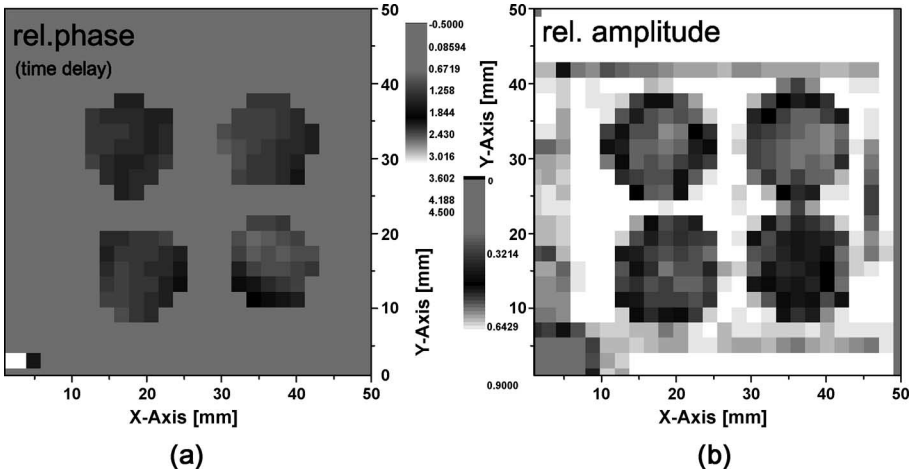

Fig. 9. *Phase and transmittance image of the sample shown in Fig. 8.*

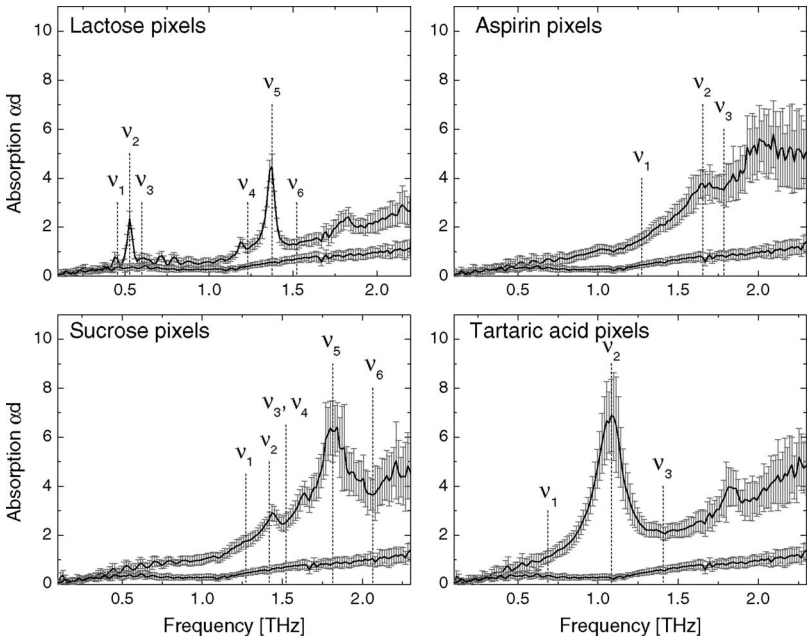

Fig. 10. *Solid lines show the average absorption of lactose (top, left), aspirin (top, right), sucrose (down, left), and tartaric acid (down, right) in the sample. The lower curve in each panel shows the absorption of the packaging material. The error bars represent one standard deviation from the mean of typically 20–30 measurements. The indicated frequencies are used for chemical recognition. After [20].*

radiation will likely find its best applications in searches for a known and limited range of possible substances.

VII. COMPLEX BIOMOLECULAR SAMPLES

Having seen that polycrystalline samples of organic molecules offer specific responses to THz radiation useful for imaging, it is of interest to apply the same techniques to larger molecules of biological relevance. Yet in contrast to the specific absorption features in the FIR spectra of crystalline biomolecules, biological systems with little or no long-range ordering of the constituent molecules exhibit little or no structure in their THz dielectric properties. Whereas the spectra of some materials like biopolymers [48] still exhibit broad weak features, most materials show featureless absorption spectra [49]. This may arise from the lack of well-defined phonon modes but also from an inhomogeneous broadening of the intramolecular vibrations. Despite of the lack of characteristic absorption features, the absorption coefficients of different samples typically still differ considerably from each other, offering potential for identification purposes. Under these conditions, if we want to compare absolute absorption values instead of characteristic fingerprint features, precise sample preparation is mandatory.

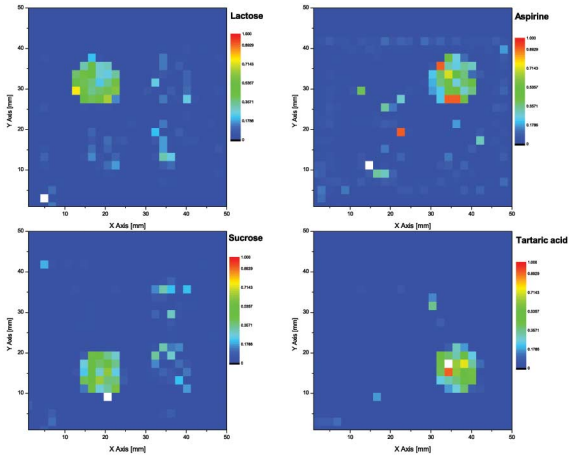

Fig. 11. *Maps of the recognition coefficient R for the four different chemicals in the sample shown in Fig. 8.*

In order to investigate the possibility to use THz imaging for identification purposes we study the influence of different sample preparation methods on reproducibility of two different RNA polymer strands, polyadenylic acid (poly-A) and polycytidylic acid (poly-C). The samples are commercially available poly-A and poly-C potassium salts (Sigma-Aldrich, product P9403 and P4903) and according to the manufacturer the molecular weight of the polymer chains is distributed between 10^5 g/mol and $2 \cdot 10^6$ g/mol, with the greatest density in the region $2 \cdot 10^5$ g/mol to $7 \cdot 10^5$ g/mol. This corresponds to polymer

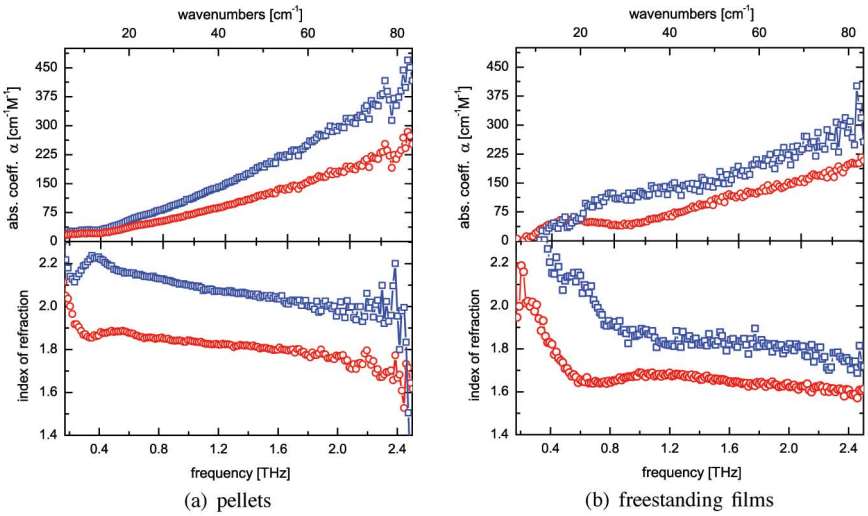

Fig. 12. *Absorption coefficient α and index of refraction of polyadenylic acid (poly-A) (circles) and polycytidylic acid (poly-C) (squares) prepared as: (a) pellets and (b) freestanding films.*

chains with lengths of approximately 600–2000 A or C units. In Fig. 12(a) we show the absorption coefficient and index of refraction (poly-A) and (poly-C) prepared as thin pellets by pressing the pure material in a die using a hydraulic press. The resulting samples were mechanically stable with thicknesses of 300 and 180 μm, respectively. The absorption coefficient of both materials increases in an almost linear fashion in the region between 0.1 and 2.5 THz. No distinct spectral features are observed. Yet poly-C absorbs stronger than poly-A at all frequencies. The index of refraction of poly-C is approximately 10% larger than that of poly-A. The strong oscillatory feature at low frequencies observed in all measurements is due to multiple reflections of the sample beam inside the relatively thin samples. We see this etalon effect only at low frequencies where the absorption is low. At higher frequencies where the absorption is substantial the THz field is absorbed before multiple reflections can occur. To avoid any artifacts arising from inappropriate sample preparation we performed additional spectroscopic measurements on poly-A and poly-C as freestanding films. These were obtained by dissolving the powder material in deionized water, distributing this solution over a 1 cm^2 area on a nonpolar polymer substrate, and lifting off the film after drying the solution by evaporation. The thicknesses of the films were in the range of 50 to 100 μm. Although we obtained slightly lower absorption coefficients, the results are in good agreement with the data obtained from spectroscopy of the pellets, particularly the overall stronger absorption of poly-C was clearly reproduced. Additional spectroscopic studies [48] performed by the group of Prof. Koch in Braunschweig, Germany, confirmed these results.

Having established that we can use THz time-domain spectroscopy to distinguish between different biopolymers, it is interesting to determine if this differentiation can be used in THz imaging as well. For this purpose we prepared targets for imaging that challenges the spatial resolution obtainable with a THz-TDS imaging system based on free-space propagation and aperture-less focusing of the THz beam. In Fig. 13 we show an image of a sample that was prepared for THz imaging by spotting small liquid volumes in a 4 × 4 array of alternating poly-A and poly-C on a TOPAS substrate. Each spot was deposited

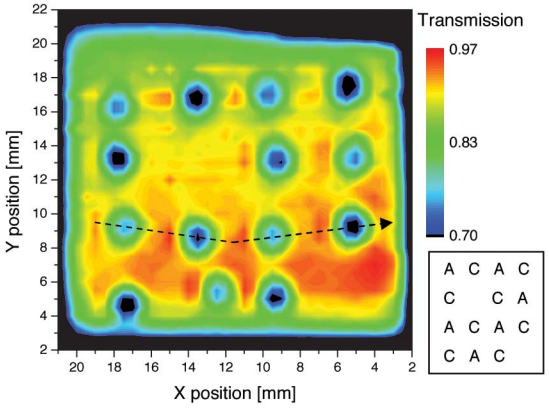

Fig. 13. *THz transmission image of a 4 × 4 spot array of poly-A and poly-C again showing stronger absorption in poly-C compared to poly-A. Each spot contained 200 μg of either poly-A or poly-C in alternating order, as indicated in the diagram to the right. The dashed line indicates the scan path of the surface profiler. After [48].*

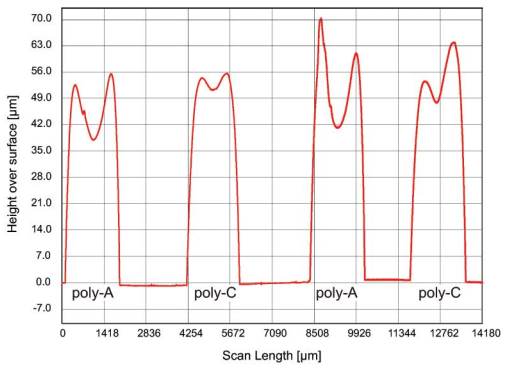

Fig. 14. *Surface height profile of the sample spots along the path indicated by the dashed line in Fig. 13. After [48].*

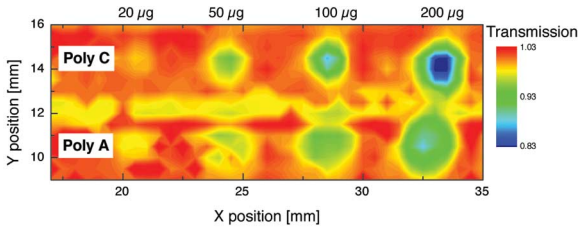

Fig. 15. *THz transmission image of a sample prepared with poly-A and poly-C spots of varying mass, ranging from 20 to 200 µg. After [48].*

with 2 μL of deionized water containing 0.2 mg material. The diameter of each spot was 1 mm. Nominally the sample consisted of a 4 $\times$ 4 array of spots, two of the spots, however, were removed from the substrate in order to identify the orientation of the substrate in the image. The spot in the top left corner of the image contains poly-A. The THz image was formed by the frequency-integrated transmission over the full bandwidth of the probe pulse. The poly-C spots lead to a substantial transmission drop of 30%, whereas the poly-A spots reduce the transmission by 20%. In order to verify that the differences observed in the image between the different spot types is related to differences in the sample material and not caused by differences in spot size or thickness we performed surface height scans with a mechanical surface profiler of the sample after the measurement.

In Fig. 14 we show the surface profile of the sample along the path indicated in Fig. 13. Notice that the horizontal scale of the plot is much smaller than the vertical scale. The spots all have approximately the same height, diameter, and topology. The average height is 40–50 μm, and the diameter is slightly larger than 1 mm. There is a pronounced height enhancement at the edges of the spots, which is normal for this type of spotting. We expect that if the topology of the spots is not similar then diffraction effects may influence the appearance of the image strongly.

Finally, we recorded a series of diluted spots as shown in Fig. 15. The sample was prepared in analogy to the sample shown in Fig. 13; however, the amount of sample material in each spot is indicated in the figure, and ranges from 20 to 200 μg. As indicated by the strong signal attenuation observed in the image of the 4 $\times$ 4 spot array in Fig. 13, we can reduce the amount of sample material by approximately an order of magnitude before the signal disappears in the present form of the experiment. The contrast between poly-A and poly-C degrades rapidly with decreasing amount of sample material.

VIII. CONCLUSION

THz detection and imaging shows great promise for identification of concealed materials and differentiation between even complex biomolecules. The techniques described in this paper can be applied in the area of quality control and security applications, since many target compounds have characteristic THz spectra while many nonmetallic nonpolar packaging materials are transparent to THz radiation. Even by relatively easy and straightforward recognition routines, it is nowadays possible to clearly identify crystalline samples by their fingerprints. More sophisticated data analysis based on pattern recognition will significantly improve the detection capability.

Yet, in contrast to crystalline samples, amorphous samples and biological systems with little or no long-range ordering of the constituent molecules exhibit little or no structure in their THz dielectric properties, due to the missing of well-defined phonon modes and inhomogeneous broadening of the intramolecular vibrations. Thus, a direct identification based on characteristic resonances seems in our opinion very difficult to perform by broadband THz imaging techniques based on free-space propagation of the THz signal. However, under controlled conditions, it may be feasible to distinguish between different biomaterials by careful determination of the absolute absorption coefficient. ■

REFERENCES

[1] A. Doria, G. P. Gallerano, E. Giovenale, G. Messina, A. Lai, A. Ramundo-Orlando, V. Spotsato, M. D'Arienzo, A. Perrotta, M. Romano, M. Sarti, M. R. Scarfi, I. Spassovsky, and O. Zeni, "THz radiation studies on biological systems at the ENEA FEL facility," *Infrared Phys. Technol.*, vol. 45, no. 5–6, pp. 339–347, 2004.

[2] E. Pickwell, B. E. Cole, A. J. Fitzgerald, V. P. Wallace, and M. Pepper, "Simulation of terahertz pulse propagation in biological systems," *Appl. Phys. Lett.*, vol. 84, no. 12, pp. 2190–2192, 2004.

[3] S. W. Smye, J. M. Chamberlain, A. J. Fitzgerald, and E. Berry, "The interaction between terahertz radiation and biological tissue," *Phys. Med. Biol.*, vol. 46, no. 9, pp. R101–R112, 2001.

[4] T. Globus, M. Bykhovskaia, D. Woolard, and B. Gelmont, "Sub-millimetre wave absorption

spectra of artificial RNA molecules," *J. Phys. D*, no. 36, pp. 1314–1322, 2003.

[5] D. L. Woolard, T. R. Globus, B. L. Gelmont, M. Bykhovskaia, A. C. Samuels, D. Cookmeyer, J. L. Hesler, T. W. Crowe, J. O. Jensen, J. L. Jensen, and W. R. Loerop, "Submillimeter-wave phonon modes in DNA macromole-cules," *Phys. Rev. E*, vol. 65, no. 5, 2002, art. no. 051 903.

[6] A. Markelz, S. Whitmire, J. Hillebrecht, and R. Birge, "THz time domain spectroscopy of biomolecular conformational modes," *Phys. Med. Biol.*, vol. 47, pp. 3797–3805, 2002.

[7] S. E. Whitmire, D. Wolpert, A. G. Markelz, J. R. Hillebrecht, J. Galan, and R. R. Birge, "Protein flexibility and conformational state: A comparison of collective vibrational modes of wild-type and D96N bacteriorhodopsin," *Biophys. J.*, vol. 85, pp. 1269–1277, 2003.

[8] R. M. Woodward, V. P. Wallace, D. D. Arnone, E. H. Linfield, and M. Pepper, "Terahertz pulsed imaging of skin cancer in the time and frequency domain," *J. Biol. Phys.*, vol. 29, pp. 257–261, 2003.

[9] Y. C. Shen, T. Lo, P. F. Taday, B. E. Cole, W. R. Tribe, and M. C. Kemp, "Detection and identification of explosives using terahertz spectroscopic imaging," *Appl. Phys. Lett.*, vol. 86, 2005, art. no. 241 116.

[10] S. Wang, B. Ferguson, D. Abbott, and X.-C. Zhang, "T-ray imaging and tomography," *J. Biol. Phys.*, vol. 29, pp. 247–256, 2005.

[11] D. Mittleman, *Sensing With Terahertz Radiation*. Berlin, Germany: Springer, 2003.

[12] M. Walther, P. Plochocka, B. Fischer, H. Helm, and P. U. Jepsen, "Collective vibrational modes in biological molecules investigated by terahertz time-domain spectroscopy," *Biopolymers*, vol. 67, no. 4–5, pp. 310–313, 2002.

[13] B. M. Fischer, M. Walther, and P. U. Jepsen, "Far-infrared vibrational modes of DNA components studied by terahertz time-domain spectroscopy," *Phys. Med. Biol.*, vol. 47, pp. 3807–3814, 2002.

[14] M. Takahashi, Y. Ishikawa, J. Nishizawa, and H. Ito, "Low-frequency vibrational modes of riboflavin and related compounds," *Chem. Phys. Lett.*, vol. 401, pp. 475–482, 2005.

[15] M. Walther, B. Fischer, M. Schall, H. Helm, and P. U. Jepsen, "Far-infrared vibrational spectra of all-trans, 9-cis and 13-cis retinal measured by THz time-domain spectroscopy," *Chem. Phys. Lett.*, vol. 332, pp. 289–295, 2000.

[16] M. Walther, B. M. Fischer, and P. U. Jepsen, "Noncovalent intermolecular forces in polycrystalline and amorphous saccharides in the far infrared," *Chem. Phys.*, vol. 288, pp. 261–268, 2003.

[17] P. C. Uphadya, Y. C. Shen, A. G. Davies, and E. H. Linfield, "Far-infrared vibrational modes of polycrystalline saccharides," *Vib. Spectrosc.*, vol. 35, pp. 139–143, 2004.

[18] P. F. Taday, I. V. Bradley, D. D. Arnone, and M. Pepper, "Using terahertz pulse spectroscopy to study the crystalline structure of a drug: A case study of the polymorphs of rantidine hydrochloride," *J. Pharm. Sci.*, vol. 92, pp. 831–838, 2003.

[19] C. J. Strachnan, T. Rades, D. A. Newham, K. C. Gordon, M. Pepper, and P. F. Taday, "Using terahertz pulsed spectroscopy to study crystallinity of pharmaceutical materials," *Chem. Phys. Lett.*, vol. 390, pp. 20–24, 2004.

[20] B. Fischer, M. Hoffmann, H. Helm, G. Modjesch, and P. U. Jepsen, "Chemical recognition in terahertz time-domain spectroscopy and imaging," *Semicond. Sci. Technol.*, vol. 20, pp. 246–253, 2005.

[21] K. Kawase, Y. Ogawa, and Y. Watanabe, "Non-destructive terahertz imaging of illicit drugs using spectral fingerprints," *Opt. Express*, vol. 11, no. 20, pp. 2549–2554, 2003.

[22] F. Huang, B. Schulkin, H. Altan, J. Federici, D. Gary, R. Barat, D. Zimdars, M. Chen, and D. B. Tanner, "Terahertz study of 1,3,5-trinitro-s-triazine (RDX) by time domain spectroscopy and FTIR," *Appl. Phys. Lett.*, vol. 83, pp. 2477–2479, 2003.

[23] Y. Chen, H. Liu, Y. Deng, D. Schauki, M. J. Fitch, R. Osiander, C. Dodson, J. B. Spicer, M. Shur, and X.-C. Zhang, "THz spectroscopic investigation of 2,4-dinitrotoluene," *Chem. Phys. Lett.*, vol. 400, pp. 357–361, 2004.

[24] L. Stryer, *Biochemistry*. New York: Freeman, 1998.

[25] M. Hineno and H. Yoshinaga, "Far-infrared spectra of mono-, di-, and tri-saccharides in 50–16 cm^{-1} at liquid helium temperature," *Spectrochim. Acta*, vol. 30, no. A, pp. 411–416, 1973.

[26] J. F. Federici, B. Schulkin, F. Huang, D. Gary, R. Barat, F. Oliviera, and D. Zimdars, "Thz imaging and sensing for security applications—Explosives, weapons and drugs," *Semicond. Sci. Technol.*, vol. 20, pp. 266–280, 2005.

[27] P. U. Jepsen and B. M. Fischer, "Dynamic range in terahertz time-domain transmission and reflection spectroscopy," *Opt. Lett.*, vol. 30, no. 1, pp. 29–31, 2005.

[28] L. F. Gervasio, G. Cardini, P. R. Salvi, and V. Schettino, "Low-frequency vibrations of all-trans-retinal: Far-infrared and raman spectra and density functional calculations," *J. Phys. Chem.*, vol. 102, pp. 2131–2136, 1998.

[29] Y. A. Grudzkov and Y. M. Gupta, "Vibrational properties and structure of pentaerythritol tetranitrate," *J. Phys. Chem.*, vol. 105A, pp. 6197–6202, 2001.

[30] J. Clarkson, W. E. Smith, D. N. Batchelder, D. A. Smith, and A. M. Coats, "A theoretical study of the structure and vibrations of 2,4,6-trinitrotoluene," *J. Mol. Struct.*, vol. 648, pp. 203–214, 2003.

[31] K. Ozeki, N. Sakabe, and J. Tanaka, "The crystal structure of thymine," *Acta Cryst. B*, vol. 25, pp. 1038–1045, 1969.

[32] M. Dauchez, P. Derreumaux, and G. Vergoten, "Vibrational molecular force field of model compounds with biologic interest: II. Harmonic dynamics of both anomers of glucose in the crystalline state," *J. Comp. Chem.*, vol. 14, pp. 263–277, 1992.

[33] M. Sekkal, P. Legrand, G. Vergoten, and M. Dauchez, "A vibrational molecular force field of model compounds with biological interest: III. Harmonic dynamics of α- and β-D-galactose in the crystalline state," *Spectrochim. Acta A*, vol. 48, pp. 959–973, 1992.

[34] G. M. Brown and H. A. Levy, "Alpha-Delta-Glucose—Further refinement based on neutron-diffraction data," *Acta Chryst. B*, vol. 35, pp. 656–659, 1979.

[35] E. Hough, S. Neidle, D. Rogers, and P. G. H. Troughton, "The crystal structure of α-D-glucose monohydrate," *Acta Cryst. B*, vol. 29, pp. 365–367, 1973.

[36] M. Yamaguchi, F. Miyamaru, K. Yamamoto, M. Tani, and M. Hangyo, "Terahertz absorption spectra of L-, D-, and DL-alanine and their application to determination of enantiometric composition," *Appl. Phys. Lett.*, vol. 86, 2005, art. no. 053 903.

[37] O. Wallach, "Zur Kenntniss der Terpene und der ätherischen Öle," *Liebigs Ann. Chem.*, vol. 286, pp. 90–143, 1895.

[38] C. P. Brock, W. B. Schweizer, and J. D. Duitz, "On the validity of Wallach rule—On the density and stability of racemic crystals compared with their chiral counterparts," *J. Amer. Chem. Soc.*, vol. 113, pp. 9811–9820, 1991.

[39] P. E. Luner, A. D. Patel, and D. C. Swenson, "(+−)-tartaric acid," *Acta Crystallographica C*, vol. 58, pp. O333–O335, 2002.

[40] B. M. Fischer, M. Franz, and D. Abbott, "T-ray biosensing: A versatile tool for studying low-frequency intermoecular vibrations," *Proc. SPIE: Biomedical Applications of Micro- and Nanoengineering III*, vol. 6416, 2006, art. no. 64 160U.

[41] H. Desseyn, K. Clou, R. Keuleers, R. Miao, V. V. Doren, and N. Blaton, "The effect of pressure and temperature on the vibrational spectra of different hydrogen bonded systems," *Spectrochim. Acta A*, vol. 57, pp. 231–246, 2001.

[42] D. H. Barker, D. T. Hodges, and T. S. Hartwick, "Far infrared imagery," *Proc. SPIE*, vol. 67, pp. 27–34, 1975.

[43] B. B. Hu and M. C. Nuss, "Imaging with terahertz waves," *Opt. Lett.*, vol. 20, pp. 1716–1718, 1995.

[44] P. U. Jepsen, M. Schall, V. Schyja, C. Winnewisser, H. Helm, and S. R. Keiding, "Detection of high power THz pulses by phase retardation in an electro-optic crystal," in *Ultrafast Processes in Spectroscopy*, Svelto *et al.*, Ed. New York: Plenum, 1996, pp. 645–648.

[45] X.-C. Zhang, Q. Wu, P. Campbell, and L. Libelo, "New field sensors for subpicosecond electromagnetic pulses," in *Ultrafast Processes in Spectroscopy*, Svelto *et al.*, Ed. New York: Plenum, 1996, pp. 649–652.

[46] B. Ferguson, S. Wang, D. Gray, D. Abbott, and X.-C. Zhang, "Identification of biological tissue using chirped probe THz imaging," *Microelectron. J.*, vol. 33, pp. 1043–1051, 2002.

[47] Y. Watanabe, K. Kawase, T. Ikari, H. Ito, Y. Ishikawa, and H. Minanide, "Component spatial pattern analysis of chemicals using terahertz spectroscopic imaging," *Appl. Phys. Lett.*, vol. 83, pp. 800–802, 2003.

[48] B. M. Fischer, M. Hoffmann, H. Helm, R. Wilk, F. Rutz, T. Kleine-Ostmann, M. Koch, and P. U. Jepsen, "Terahertz time-domain spectroscopy and imaging of artificial RNA," *Opt. Express*, vol. 13, no. 14, pp. 5205–5215, 2005.

[49] J. Knab, J. Y. Chen, and A. G. Markelz, "Hydration dependence of confirmational dilectric relaxation of lysozyme," *Biophys. J.*, vol. 90, no. 7, pp. 2576–2581, 2006.

ABOUT THE AUTHORS

Bernd M. Fischer was born in Waldkirch, Germany. In 1997/98 he studied for one year in Paris where he completed a Stage de Maitrise in biophysics from the IPB, University Paris XI, France, in 1998 and the Diplom degree (with distinction) and the Ph.D. degree (*summa cum laude*) in physics from the University of Freiburg, Germany in 2001 and 2006, respectively.

In 2006, he joined the Adelaide T-ray Group, University of Adelaide, Adelaide, Australia, and in 2007 he received an Australian Research Council (ARC) Australian Postdoctoral (APD) Fellowship.

Hanspeter Helm was born in Austria. He received the Ph.D. degree from the University of Innsbruck, Austria, in 1973.

Following a postdoctoral fellowship at the Australian National University, Canberra, Australia, he joined SRI International in 1978. Since 1994, he has been the Head of the Department of Molecular and Optical Physics, University of Freiburg, Freiburg, Germany.

Dr. Helm is a Fellow of the American Physical Society.

Peter Uhd Jepsen was born in Denmark. He received the Ph.D. degree from Aarhus University, Denmark, in 1996.

He joined the group of Hanspeter Helm at the University of Freiburg, first as a Postdoctoral Fellow (1996–1998) and then as Assistant Professor (1998–2004). He received the Habilitation degree in 2003. Since 2005 he is Associate Professor at the Department of Materials, Optics, and Communications at the Technical University of Denmark, Kongens Lyngby, Denmark.